

# Bounding-box Watermarking: Defense against Model Extraction Attacks on Object Detectors

Satoru Koda  
Fujitsu Limited, Japan  
koda.satoru@fujitsu.com

Ikuya Morikawa  
Fujitsu Limited, Japan  
morikawa.ikuya@fujitsu.com

## Abstract

Deep neural networks (DNNs) deployed in a cloud often allow users to query models via the APIs. However, these APIs expose the models to model extraction attacks (MEAs). In this attack, the attacker attempts to duplicate the target model by abusing the responses from the API. Backdoor-based DNN watermarking is known as a promising defense against MEAs, wherein the defender injects a backdoor into extracted models via API responses. The backdoor is used as a watermark of the model; if a suspicious model has the watermark (i.e., backdoor), it is verified as an extracted model. This work focuses on object detection (OD) models. Existing backdoor attacks on OD models are not applicable for model watermarking as the defense against MEAs on a realistic threat model. Our proposed approach involves inserting a backdoor into extracted models via APIs by stealthily modifying the bounding-boxes (BBs) of objects detected in queries while keeping the OD capability. In our experiments on three OD datasets, the proposed approach succeeded in identifying the extracted models with 100% accuracy in a wide variety of experimental scenarios.

## 1. Introduction

Deep neural networks (DNNs) are often designed to operate in a cloud and offer prediction APIs. Clients can obtain model predictions on their data via the APIs. However, such DNNs are vulnerable to model extraction attacks (MEAs) [24], whose objective is to extract a function-similar duplicate of a target model. High-performance DNNs constitute valuable intellectual properties. Additionally, some APIs (e.g. OpenAI API) explicitly prohibit using API responses to train competing models [2]. Thus, AI service providers need to address the threat posed by MEAs.

Model watermarking has garnered considerable attention as a defense measure against MEAs [26, 29]. Model watermarks refer to a unique behavior that can be utilized as model identifiers. Given an input, suppose that only one

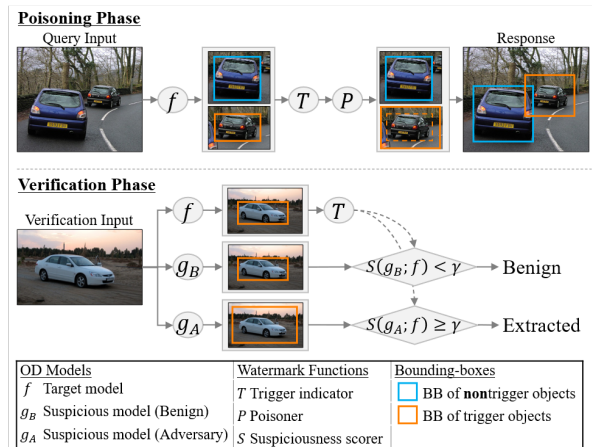


Figure 1. Overview of proposed model watermarking approach. The poisoning phase modifies the BBs of the objects containing a predefined trigger to inject a backdoor into extracted models. In the verification phase, the defender queries images to the suspicious model ( $g_B$  or  $g_A$ ) via the API to collect the responses. If the suspicious model contains the backdoor, which is a model behavior outputting distorted (e.g. expanded) BBs only on objects with the trigger, the model is judged as an extracted model.

model outputs prediction A, while others output prediction B. Then, the model becomes identifiable owing to the unique prediction to the input. In recent years, backdoor-based watermarking has been substantially explored [3, 11–13, 18, 22]. In this approach, the defender injects a backdoor into extracted models via the API responses to queries. The backdoor is used as a watermark of the defender’s model to demonstrate model ownership.

This work focuses on backdoor-based watermarking for object detection (OD) models. Although backdoor attacks on OD models have been proposed [5, 6, 15–17], they are not applicable for model watermarking as the defense against MEAs due to the following reasons. (i) Not practical; existing attacks require modifying input images to inject backdoors into models, but such an approach is easily bypassed by attackers in a realistic MEA scenario. (ii)

Not stealthy; existing attacks require drastically modifying API responses to inject backdoors, implying that ME attackers can perceive the backdooring process. (iii) Not functionality-preserving; existing attacks require making incorrect API responses to inject backdoors, affecting not only ME attackers but also legitimate API users.

Herein, we present a backdoor-based watermarking approach termed *bounding-box watermarking (BBW)* to address the aforementioned three challenges, whose overview is figured in Fig. 1. Given a queried image, BBW intentionally poisons (e.g., expands) object BBs while maintaining the OD functionality. Poisoning is only applied to objects with a predefined trigger. The poisoned API responses induce a backdoor to extracted models. To demonstrate model ownership verification, the model owner verifies if a suspicious model contains the intended backdoor, which is a behavior unique to extracted models that returns odd BBs only to objects with the predefined trigger. In our experiments, BBW identified extracted models with 100% accuracy in many experimental scenarios. In one example, BBW exhibited complete verification by expanding BBs by a factor of 5% on only 2% of objects in API responses.

**Contribution** We are the first to present a backdoor-based watermarking approach as a defense measure against MEAs on OD models. The approach is practical, stealthy, and functionality-preserving.

## 2. Background

**Object Detection (OD)** Given an input image, an OD model outputs the object category and the coordinates of the BB for each object in the image. Let  $\mathbf{x} \in \mathcal{X}$  be an input image of the size  $W$  (width)  $\times H$  (height) and  $f : \mathcal{X} \rightarrow \mathcal{O}^L$  be an object detector, where  $\mathcal{O}$  is an object space. The prediction  $f(\mathbf{x}) = \{o_f^l\}_l$  is a set of the objects detected in  $\mathbf{x}$  by  $f$ . Each object  $o_f^l$  is denoted as

$$o_f^l = (c_f^l, bb_f^l), \quad (1)$$

where  $c_f^l \in \mathbb{N}$  denotes the object category, and  $bb_f^l = (a_f^l, b_f^l, w_f^l, h_f^l) \in \mathbb{R}^4$  denotes the BB coordinate. Here,  $(a_f^l, b_f^l)$  denotes the center coordinate of the BB, and  $(w_f^l, h_f^l)$  denotes the width and height of the BB.

**Model Extraction Attack (MEA)** Suppose that a target model is operating in a cloud and offering a prediction API. MEAs aim at extracting the target model [24]. The attacker queries a substitute set  $\{\mathbf{x}_i\}_i$  to the target model  $f$  via the API and obtains the annotations  $\{f(\mathbf{x}_i)\}_i$  on the set. Subsequently, the attacker trains a model using the annotated substitute data  $\{(\mathbf{x}_i, f(\mathbf{x}_i))\}_i$ . Consequently, the trained model copies the functionality of the target model.

**DNN Watermarking** DNN watermarking employs a unique behavior of a DNN as a model indicator [26, 29]. Adi *et al.* [3] leveraged backdoor attacks for DNN watermarking. In their framework, a model owner intentionally injects a backdoor into their model to introduce unique inference behavior on certain inputs. Then, the unique behavior is used as a model watermark.

## 3. Related Work

### 3.1. Watermarking as a Defense against MEAs

Recent studies have further utilized the backdoor-based watermarking as a defense against MEAs. The owner of an attack target model (*i.e.*, defender) designs the API so that the extracted models contain a backdoor. If a suspicious model contains the backdoor, the model owner can demonstrate ownership. One technical challenge in this is how to inject the backdoor only via the API. The approaches are split into the following two categories according to the poisoning targets: *model poisoning* and *response poisoning*. The approaches in the former category intentionally poison the target model to make it contain a backdoor that is transferable to the extracted models [12, 13]. Whereas, the approaches in the response poisoning category do not poison target models but API responses [18, 22]. Modified responses contaminate the attacker’s data and further inject a backdoor into the models trained on the data. This work focuses on the response poisoning approach. Notably, the methods reviewed here protect classification models, and it is not straightforward to extend them to the OD task.

### 3.2. Backdoor Attacks on Object Detectors

Here, we review existing work of backdoor attacks against OD and then discuss their applicability to backdoor-based watermarking against MEAs.

**Existing Attacks** Chan *et al.* [5] proposed BadDet, wherein the attacker puts a trigger patch on images and trains a backdoored model so that the trigger achieves attack objectives, such as erasing BBs or flipping object categories. Luo *et al.* [15] adopted a similar approach. Chen *et al.* [7] extended BadDet; they realized a clean-label backdoor attack by adjusting the position of a trigger patch put on images. Ma *et al.* [16] demonstrated a backdoor attack with a natural trigger. Specifically, they treated persons wearing a specific blue T-shirt as a trigger. Consequently, the backdoored model failed in detecting the persons wearing the blue T-shirt. Ma *et al.* [17] showed the effectiveness of the image scaling attack [28] on OD models. In this attack, a poisoning object appears only when the image is resized to be fed into DNNs. Chen *et al.* [6] defined a natural trigger based on a combination of objects; if a specific combination arises in a single image, the backdoor is

	Poisoning Target			Properties		
	Input ( $x$ )	Label ( $c$ )	BB ( $bb$ )	P	S	FP
Chan <i>et al.</i> [5]	✓	✓	✓			
Luo <i>et al.</i> [15]	✓		✓			
Chen <i>et al.</i> [7]	✓				✓	✓
Ma <i>et al.</i> [16]			✓	✓		
Ma <i>et al.</i> [17]	✓				✓	✓
Chen <i>et al.</i> [6]		✓	✓	✓		
Snarski <i>et al.</i> [21]	✓				✓	✓
<b>This work</b>			✓	✓	✓	✓

Table 1. Summary of existing backdoor attacks on OD models and their applicability to model watermarking. **P**, **S**, and **FP** respectively denote practicality, stealth, and functionality preservation.

activated. All the above-mentioned works primarily aim at attack demonstration. With regard to backdoor attacks on OD for defense purposes, no study has been conducted except by Snarski *et al.* [21]. However, their watermarking target is not a model but a dataset. The model trained on the watermarked dataset is induced to contain a backdoor.

**Applicability of Existing Attacks to Watermark** Table 1 summarizes whether the existing backdoor attacks are applicable to backdoor-based watermarking for the defense purpose against MEAs. Specifically, we discuss if they hold the following properties: (**P**) practicality—the attack can inject a backdoor (*i.e.* watermark) into extracted models in a realistic threat model, (**S**) stealth—the attack is undetectable by ME attackers, and (**FP**) functionality preservation—the attack does not affect legitimate API users.

Backdoor attacks involving “input” modification are impractical, such as the patch attacks [5, 7, 15, 21] and the image rescaling attack [17], because ME attackers have clean images. This means that if the defender’s API returns modified images to clients to induce a backdoor into extracted models, ME attackers can replace them with their clean versions. Additionally, the backdoor attacks involving drastic changes in outputs, such as changing object categories or erasing BBs [5, 6, 15, 16], are not stealthy. ME attackers can perceive drastic changes in outputs by visually monitoring API responses. Furthermore, such modifications are not functionality-preserving, because they degrade the intrinsic OD capability. Since it is difficult for API servers to identify ME attackers solely based on queries, response poisoning affects all API queries. Thus, poisoning must have the least impact on legitimate users. Our approach addresses these challenges.

## 4. Problem Formulation

**Assumption** The defender (*i.e.*, model owner/victim) makes an OD model  $f$  available via an API, where  $f$  is subject to the target of MEAs. To a queried image  $x$ , the API returns the five-dimensional vectors of the detected objects,

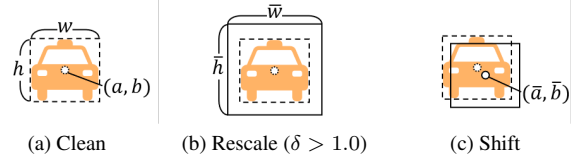


Figure 2. BB poisoning patterns

each of which comprises the object label  $c$  and the BB coordinate  $bb$  (Eq. (1)). We assume that the internal information of models cannot be accessed by any outsider.

**Threat Model** The attacker’s goal is to obtain an extracted model  $g$  whose functionality is sufficiently similar to that of the target model  $f$ . They cannot acquire the training data of  $f$ , but they can collect substitute data of the target domain. They obtain the OD results on the data by querying  $f$  and treat them as the ground truth for training the extracted model  $g$ . Once  $g$  is trained, the attacker releases the API of the model because, as noted by Szyller *et al.* [22], it has the greatest impact on the attack target. This threat model is the same as the one used in Szyller *et al.* [22] except for the recognition task (classification  $\rightarrow$  OD).

**Defense by Watermarking** The defender’s goal is to plant a watermark into extracted models so that the defender can claim that an MEA is performed. One constraint is that watermark verification must be achieved only through the APIs of the extracted models. To explain more formally, let  $f_w \in \mathcal{F}$  be a watermarked model and  $f_n \in \mathcal{F}$  be a non-watermarked model, where  $\mathcal{F}$  denotes the space of functions. For watermark verification, the defender defines the following two items: *key-set*  $\mathcal{D}_{key}$ , an image set used for the verification, and a *verification logic*  $S$ . Specifically,  $S$  outputs a scalar score on any set of OD predictions. The logic  $S$  is said to be *verifiable* if it satisfies the following condition:

$$S(f_w(\mathcal{D}_{key})) > S(f_n(\mathcal{D}_{key})) \text{ for } \forall f_w, \forall f_n \in \mathcal{F} \quad (2)$$

The defender must design an API such that any watermarked extracted model is verifiable by  $S$  on  $\mathcal{D}_{key}$ .

## 5. Proposed Approach

This section describes our proposed defense approach, BBW, which comprises two phases, poisoning and verification. The overview is figured in Fig. 1.

### 5.1. Poisoning Phase

This phase modifies (*i.e.*, poisons) responses to queries to induce a backdoor into extracted models.

As a preparation, the defender first defines a *trigger*, which is an object characteristic. We refer to the objects

containing the trigger as *trigger objects*. Our trigger selection strategy is presented at the end of this section. Once the defender’s API receives an input  $x \in \mathcal{X}$ , the target model  $f$  executes OD. Thereafter, poisoning is only applied to the trigger objects. This procedure is represented with a *poisoner*  $P : \mathcal{O} \rightarrow \mathcal{O}$  as  $P(o)$ , where  $o$  is a trigger object.

We present a concrete poisoning procedure. Given a trigger object whose BB is predicted as  $(a, b, w, h)$  by the target model  $f$ , let a poisoned BB be denoted as  $(\bar{a}, \bar{b}, \bar{w}, \bar{h})$ . The poisoner  $P$  modifies the predicted BB as

$$\bar{w} = \delta_w \cdot w \quad (\delta_w \in (0, W/w]), \quad (3)$$

$$\bar{h} = \delta_h \cdot h \quad (\delta_h \in (0, H/h]), \quad (4)$$

while  $\bar{a} = a$  and  $\bar{b} = b$ . This procedure is visualized in Fig. 2b. We call the parameter  $\delta_*$  *poisoning magnitude*.

**Significance** Our watermark with the proposed poisoning pattern can satisfy the three properties mentioned above, *i.e.*, practicality, stealth, and functionality preservation. First, our approach works under the realistic threat model assumed in Sec. 4 because the poisoning is not applied to queried images but to query responses. Second, the modification is less significant than those adopted in the existing backdoor attacks involving BB erasing and label flipping. Lastly, the modification is functionality-preserving. Suppose that  $\delta_w$  and  $\delta_h$  are both greater than 1.0. As BBs still surround objects, the OD functionality will be kept. In this sense, the poisoning with a poisoning magnitude greater than 1.0 is more functionality-preserving than that with a poisoning magnitude less than 1.0 or poisoning procedures involving a BB shift. (Fig. 2c).

## 5.2. Verification Phase

This phase verifies if a suspicious model  $g$  is an extraction of the target  $f$ . In short, we leverage the watermark such that backdoored extracted models output odd BBs only to trigger objects.

**Key-set Preparation** The defender first prepares a verification dataset  $\mathcal{D}_{key}$  that contains both trigger and nontrigger objects. Then, the defender collects the outputs of the two models  $f$  and  $g$  on  $\mathcal{D}_{key}$  via their respective APIs. Further, among all the objects predicted by  $f$ , the defender configures a subset  $\mathcal{U}$ ; the object  $o$  in  $\mathcal{U}$  is assumed to be detected by both  $f$  and  $g$  as the same object. Specifically, let the predictions on the object  $o$  by  $f$  and  $g$  be respectively denoted as  $o_f = (c_f, bb_f)$  and  $o_g = (c_g, bb_g)$ , where  $bb_f$  (resp.  $bb_g$ ) is denoted as  $(a_f, b_f, w_f, h_f)$  (resp.  $(a_g, b_g, w_g, h_g)$ ). Any object in  $\mathcal{U}$  must meet the following condition:

$$\{c_f = c_g\} \wedge \{\text{IoU}(bb_f, bb_g) > \eta\}, \quad (5)$$

where  $\text{IoU}(\cdot, \cdot)$  computes the Intersection of Union (IoU) between the two BBs, and  $\eta$  is a predefined threshold to

assure that the BBs sufficiently overlap. Finally,  $\mathcal{U}$  is split into  $\mathcal{V}$  and  $\mathcal{V}^c$ , which are respectively the sets of the trigger and the nontrigger objects ( $\mathcal{V} \cup \mathcal{V}^c = \mathcal{U}$ ).

**Suspiciousness Score** Once  $\mathcal{D}_{key}$  is prepared, the defender computes the degree of suspiciousness of model  $g$ , called *suspiciousness score*, as

$$S(g(\mathcal{D}_{key}); f) = \frac{\sum_{o \in \mathcal{V}} d(o_f, o_g) / |\mathcal{V}|}{\sum_{o \in \mathcal{V}^c} d(o_f, o_g) / |\mathcal{V}^c|}. \quad (6)$$

Here,  $d(o_f, o_g)$  measures the inconsistency of the predictions on  $o$  by  $f$  and  $g$ , which we call *prediction inconsistency*. The possible options for  $d(o_f, o_g)$  are as follows:

$$d_{\text{IoU}}(o_f, o_g) = 1 - \text{IoU}(bb_f, bb_g), \quad (7)$$

$$d_{\text{scale}}(o_f, o_g) = \left(\frac{w_g}{w_f}\right)^{\text{sgn}(\delta_w - 1)} \times \left(\frac{h_g}{h_f}\right)^{\text{sgn}(\delta_h - 1)}. \quad (8)$$

These metrics become large as the BBs predicted by the two models are inconsistent. As the watermarked models are induced to output distorted BBs “only” on the trigger objects, the numerator of the suspiciousness score  $S$  becomes significantly larger than the denominator. Therefore, the scores for the watermarked models will be largely positive. To the contrary, the scores for nonwatermarked models will be around 1.0. Consequently, the score  $S$  becomes a *verifiable* watermarking verification logic (Eq. (2)).

## 5.3. Trigger Selection

This subsection explains how to define a trigger and an indicator function  $T : \mathcal{O} \rightarrow \{0, 1\}$  that returns whether an object  $o \in \mathcal{O}$  has the trigger or not.

**Key Idea** We execute clustering analysis on the objects in the training set and then select one cluster. We refer to the selected cluster as the *trigger cluster*. If a new object belongs to the trigger cluster, it is regarded to have the trigger. This strategy must be stealthy because the trigger is not described with explicit object characteristics.

We believe that the cluster should be as compact as possible. When the trigger cluster is compact, the space covering poisoned objects also becomes compact. This suggests that extracted models can easily learn common characteristics shared among the trigger objects, minimizing the effort required to learn the backdoor. This cluster design also makes the backdoor robust to countermeasures for backdoor elimination. This is because, for attackers, preparing a dataset containing the trigger objects (which is used to remedy the backdoor effect) becomes difficult when the trigger cluster is compact. Thus, the cluster should be compact.

---

**Algorithm 1** Trigger Cluster Search

---

**Input:** poisoning ratio  $p$ , feature matrix  $Z \in \mathbb{R}^{n \times m}$ , search tolerance  $t$ , search step  $\delta_\varepsilon$

**Output:**  $\bar{\varepsilon}, \bar{Z}$

```
1:  $\varepsilon \leftarrow 0, cond \leftarrow \text{False}$ 
2: while not  $cond$  do
3:    $C = \text{DBSCAN}(\varepsilon).fit(Z)$            #  $C$ : set of clusters
4:   Get  $C \in C$                          # cluster with the most data
5:   if  $|\text{size}(C) - n \cdot p| < t$  then
6:      $cond \leftarrow \text{True}$ 
7:   else
8:      $\varepsilon \leftarrow \varepsilon + \delta_\varepsilon$ 
9:   end if
10: end while
11:  $\bar{\varepsilon} \leftarrow \varepsilon, \bar{Z} \leftarrow Z_C$  #  $Z_C$ : feature matrix of the objects in  $C$ 
12: return  $\bar{\varepsilon}, \bar{Z}$ 
```

---

**Trigger Cluster Search** We present a search algorithm to find the most compact cluster. Assume that a training set containing  $n$  objects is given. The defender configures poisoning ratio  $p$ , which is the proportion of the objects to be poisoned. The search algorithm comprises the following three steps. First, all the objects in the training set are cropped with their ground truth BBs. Second, the feature vectors of the cropped objects are extracted using a feature extractor  $E : \mathcal{O} \rightarrow \mathbb{R}^m$ , composing the feature matrix  $Z \in \mathbb{R}^{n \times m}$ . Third, DBSCAN [9] is applied to  $Z$  to search the most compact cluster containing  $n \times p$  samples.

We now present the details of the step 3. Given a parameter  $\varepsilon (> 0)$ , DBSCAN groups the neighbor samples within the distance of  $\varepsilon$ . The grouped samples compose a cluster. Thus if  $\varepsilon$  is too small, every sample composes individual clusters. Following this principle, the search process starts with a small  $\varepsilon$ . Then, DBSCAN is repeatedly applied to  $Z$  while gradually increasing  $\varepsilon$  until the largest cluster (*i.e.*, cluster with the most data) contains approximately  $n \times p$  samples. Once such a cluster is found, it is regarded as the trigger cluster. The defender retains the parameter  $\bar{\varepsilon}$  found during this process and the set of feature vectors of the objects belonging to the trigger cluster, denoted as  $\bar{Z}$ . The pseudo code of this process is presented in Algorithm 1.

**Trigger Indicator** The defender defines the union of the  $\bar{\varepsilon}$ -balls of the trigger objects as  $\mathcal{B} = \cup_{\bar{z} \in \bar{Z}} \{z \in \mathbb{R}^m | \text{dist}(z, \bar{z}) < \bar{\varepsilon}\}$  and the trigger indicator function  $T$  as:  $T(o) = 1$  if  $E(o) \in \mathcal{B}$  and 0 otherwise. Once the target API receives a query, it determines the responses to be poisoned as follows: (i)  $f$  conducts OD, (ii) the detected objects are cropped with their predicted BBs, (iii)  $E$  extracts the features of the cropped objects, and (iv)  $T$  evaluates if each of the objects should be poisoned.

## 6. Experiments

### 6.1. Settings

**Datasets** We used three OD datasets, PascalVOC2007 (VOC07) [10], Self-Driving Cars–TrafficSigns [4], and CityPersons [30]. Their details and dataset statistics are explained in Appendix:A.1. Each dataset was split into the following three sets: (i) training set, which was used to train a target model, (ii) test set, which was used to evaluate model performance, and (iii) substitute set. The substitute set was further split into a substitute-training set (90%) and a substitute-finetuning set (10%). The former was used for training extracted models and benign models. The latter was used to finetune the extracted models to evaluate the robustness of our watermark. The key-set  $D_{key}$  was configured from either of the training or the test set for each dataset, whose setup details are written in Appendix:A.2.

**Models** First, we trained a target model on the training set. Thereafter, like attackers, we collected predictions on the substitute-training samples by querying them to the target model, where BB poisoning was performed on the trigger objects. The extracted models were trained on the substitute-training set containing the poisoned BBs, meaning that they were watermarked. Besides, benign models were trained on the substitute-training set with ground truth annotations. As a baseline, we trained **non**watermarked extracted models, which we refer to as baseline models. The baseline models were trained on the **un**poisoned responses by the target model. We adopted the Ultralytics-YOLOv8s model for the target models and the Ultralytics-YOLOv8n model for the other models [27]. Their hyperparameter settings are explained in Appendix:B.1. We measured OD performance of the models using mAP50. The performance table is presented in Appendix:B.2.

**Poisoning Configuration** We adopted the rescale-based BB poisoning (Eqs. (3) and (4)) and the suspiciousness score  $S$  based on the scale-based inconsistency metric (Eq. (8)). For the poisoning magnitudes ( $\delta_w, \delta_h$ ), we assumed that  $\delta_w = \delta_h (= \delta)$ , and the newly introduced  $\delta$  was configured in  $\{0.8, 0.9, 0.95, 1.05, 1.1, 1.2\}$ . The poisoning ratio  $p$  was varied in the following sets: VOC07 and TrafficSigns,  $\{1\%, 2\%, 3\%\}$ ; and CityPersons,  $\{1\%, 3\%, 5\%\}$ . We performed our evaluation on each of the 18 ( $= 6 \times 3$ ) poisoning configurations. We used EfficientNet-B4 [23] as the object feature extractor  $E$ . The statistics of the trigger objects and the key-set for each configuration are presented in Appendix:C.1 and C.2, respectively. The OD performance by the extracted models is shown in Appendix:C.3.

**Evaluation Criterion for Watermark** We trained 30 benign models and 30 extracted models for each poisoning

Dataset	Ratio	Poisoning Magnitude							
		0.8	0.9	0.95	1.0	1.05	1.1	1.2	
VOC07	1%	91.56	78.67	63.22	30.56	43.44	51.67	66.67	
	2%	100.0	100.0	100.0	7.78	100.0	100.0	100.0	
	3%	100.0	100.0	100.0	30.56	100.0	100.0	100.0	
TrafficSigns	1%	93.44	92.56	94.11	12.11	20.11	52.11	95.11	
	2%	100.0	92.78	93.56	35.78	71.78	94.56	100.0	
	3%	100.0	100.0	96.67	38.11	90.89	99.89	100.0	
CityPersons	1%	26.56	21.78	25.11	81.22	76.67	79.44	75.89	
	3%	85.22	83.56	74.89	52.22	72.67	79.11	83.67	
	5%	83.22	69.22	50.56	87.11	96.44	99.0	99.89	

Table 2. Watermark verification accuracy (AUROC, %) using BBW. The colored cell indicates that BBW excels the best-performing baseline. The results with the IoU-based inconsistency metric are reported in Appendix:D.1.

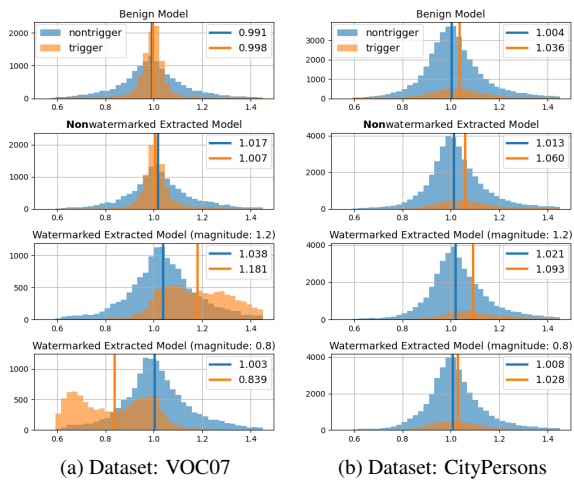


Figure 3. Histograms of scale-based prediction inconsistency between the target model and: (top) the benign models, (second) the baseline models, (third) the extracted models with  $\delta = 1.2$ , and (fourth) the extracted models with  $\delta = 0.8$ . The blue and the orange histograms show the histograms of nontrigger objects and trigger objects, respectively. Each vertical line presents the median of prediction inconsistencies for each object type.

configuration with different seeds. We evaluated the *verification accuracy* for watermark evaluation using the binary classification AUROC of the benign/extracted models based on the suspiciousness score  $S$ .

## 6.2. Results

**Quantitative Results** Table 2 presents the results, where the column with the poisoning magnitude of 1.0 indicates the results for the baseline models. Hereafter, we closely review the results for each dataset.

**VOC07.** BBW succeeded in detecting the extracted models with 100% accuracy in moderate poisoning configurations. For instance, BBW could perform complete verification just by expanding BBs by a factor of 5% on only

2% of the detected objects. This implies that our approach is difficult to perceive. Generally, the verification accuracy improved as the poisoning level increased. Figure 3a shows the distributions of prediction inconsistencies (or more precisely,  $\frac{w_g \cdot h_g}{w_f \cdot h_f}$ ) for the models of each type. For the benign and the baseline models, there is no clear difference in the distributions between trigger and nontrigger objects. Their distributions are distributed around 1.0, meaning that the predictions by the target model and the benign/baseline models are almost consistent on both trigger and nontrigger objects. For the watermarked extracted models, in contrast, only the distribution of trigger objects is shifted to the left or the right depending on the poisoning magnitudes. Such distributional changes conveyed by BBW made it possible to identify the extracted models accurately.

**TrafficSigns.** Although stronger poisoning configurations were required on this dataset than on the VOC07 dataset, BBW still achieved complete verification in many settings. Hereafter, we do not analyze the results on this dataset deeply because the overall tendency of the results was similar to that of the results on the VOC07 dataset.

**CityPersons.** BBW was still able to perform nearly complete verification by expanding BBs by a factor of 20% on 5% (or more precisely, 3.55%) of the detected objects. Different from the cases for the other datasets, our watermark verification logic performed reasonably even without BB poisoning (AUROC 87.11%). This result stemmed from the fact that only the baseline models unintentionally have learned the tendency to output relatively large BBs on the trigger objects. This can be confirmed in the top two figures of Fig. 3b; only the prediction inconsistency distribution on the trigger objects of the baseline models (the orange histogram in the second figure) is shifted to the right, when compared to that of the benign models. However, this phenomenon is not controllable by the defenders. Nonetheless, our BB poisoning made the unintentional backdoor more significant. Comparing between the second and the third figure of Fig. 3b, the prediction inconsistency on the trigger objects was amplified by our BB poisoning (1.060  $\rightarrow$  1.093), while that on the nontrigger objects was not changed much (1.013  $\rightarrow$  1.021). This increased gap contributed to making the watermark verification more accurate. On the other hand, the poisoning with the magnitudes less than 1.0 did not work, because the BB rescaling acted in a way that the poisoning offsets the unintentional backdoor effect, which can be confirmed from the bottom figure of Fig. 3b.

**Qualitative Results** *Watermark Visualization.* Figure 4 shows examples of detection results by the models of each type. It is visible that only the watermarked model predicts expanded BBs just on the trigger objects (depicted with orange rectangles). Note that we dared to use a strong poisoning magnitude in these examples just for better visibility.

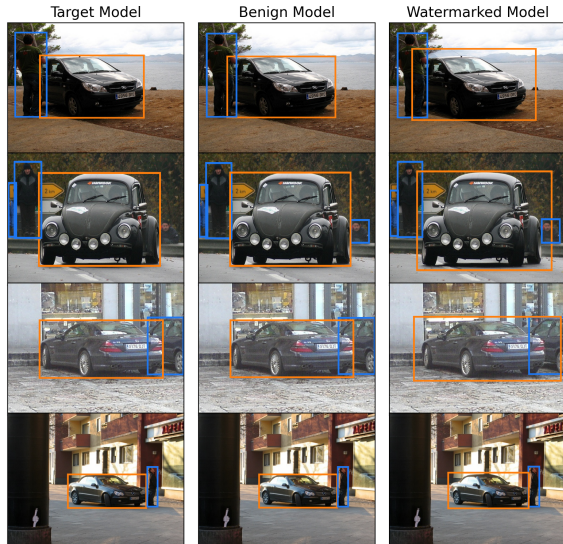


Figure 4. Visualization of our proposed watermark on the VOC07 dataset. The figures in the first, second, and third column display prediction examples by the target, a benign, and a watermarked extracted model ( $\delta = 1.2$ ), respectively. The orange BBs indicate that the object is a trigger object. See Appendix:D.2 for visualization results for the other two datasets.

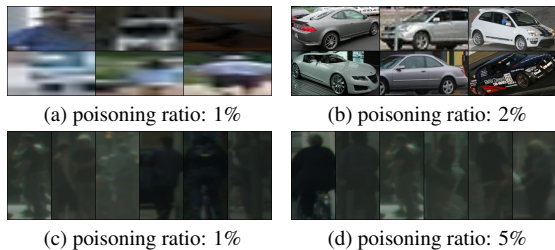


Figure 5. Trigger objects in (a,b) VOC07 and (c,d) CityPersons.

*Trigger Objects Visualization.* Figure 5 visualizes examples of the trigger objects. For the VOC07 dataset, when the poisoning ratio is 1%, the trigger objects are very coarse and do not have sufficient information. This is perhaps the reason of the failure of watermark verification. When the poisoning ratio is 2%, the trigger objects seem to have common features (“compact cars”). Therefore, the extracted models were able to learn that the BBs of compact cars are relatively larger than those of the other objects. For the CityPersons dataset, the trigger objects are coarse but barely identifiable as persons or riders in dark environment. This is why the watermark verification was more challenging on the dataset than on the VOC07 dataset. Besides, there is no significant change in the appearance of the trigger objects in all the poisoning ratios. This is the reason why the watermark verification performances were improved gradually as the poisoning levels increased.

Dataset	Ratio	Poisoning Magnitude		
		1.05	1.1	1.2
		random / compact		
VOC07	2%	97.78 / <b>100.0</b>	<b>100.0 / 100.0</b>	<b>100.0 / 100.0</b>
TrafficSigns	3%	81.44 / <b>90.89</b>	98.11 / <b>99.89</b>	<b>100.0 / 100.0</b>
CityPersons	5%	88.44 / <b>96.44</b>	98.44 / <b>99.0</b>	99.56 / <b>99.89</b>

Table 3. Watermark verification accuracy (AUROC, %) with the random and the compact cluster. The distributions of the trigger objects of both clusters are visualized in Appendix:E.1.

## 7. Analysis and Discussion

We discuss the effectiveness of our trigger selection in Sec. 7.1, the transferability of our watermark in Sec. 7.2, and the robustness of our watermark in Sec. 7.3.

### 7.1. Ablation: Trigger Cluster Selection

Our intuition for a good trigger is that the space covering trigger objects should be as compact as possible so that extracted models can easily learn common characteristics shared among the trigger objects. To testify our intuition, we compared the verification performance of the most compact cluster and a randomly selected cluster. As a setup for the random cluster, we randomly sampled objects from the training set at a given poisoning ratio  $p$ . Then, we adjusted the parameter  $\bar{\epsilon}$  so that the union of the  $\bar{\epsilon}$ -balls contains approximately  $n_{sub} \times p$  objects in the substitute-training set, where  $n_{sub}$  is the number of objects in the set. The results of this ablation study are presented in Table 3. The compact cluster universally outperformed the random cluster.

### 7.2. Watermark Transferability

**Non-i.i.d. Data** We assume a non-i.i.d. scenario where attackers cannot access to the training distribution. Specifically, the target model was trained on VOC07 while the attacker used the COCO minitrain data [1] as the substitute data.<sup>1</sup> The results were as follows: the verification accuracy was 4.0%, 100.0%, and 100.0% at poisoning ratios of 1% (0.60%), 3% (0.63%), and 5% (2.72%), respectively, where  $\delta$  was set to 1.1. Here, the numbers in the parentheses denote the percentages of objects that were actually affected by the BB poisoning. Although there existed a gap between the given poisoning ratio (e.g., 5%) and the actual poisoning ratio (e.g., 2.72%), BBW achieved complete verification.

Unfortunately, these results suggest that as the gap increases, stronger poisoning is necessary. Ultimately, when the distributions of the training and the substitute data are not overlapped, BBW will fail in watermarking because no query responses will be poisoned. In general, MEAs using out-of-distribution data, called data-free MEAs [25], are not as promising as those using in-distribution data. However,

<sup>1</sup>We did not perform experiments on the other two datasets, because their label sets are not fully covered by the COCO minitrain dataset.

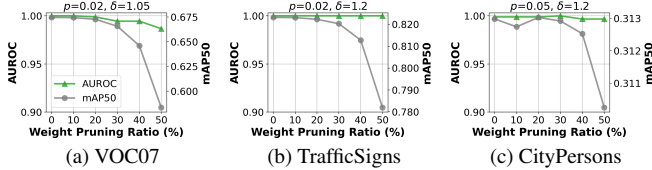


Figure 6. Watermark robustness to weight pruning.

the literature has demonstrated that such attacks are possible against classification models. Hence, protecting OD models from data-free MEAs by BBW is our future work.

**Other OD Model** So far we assumed that the attacker used a nearly identical model architecture (YOLOv8n) to the target model (YOLOv8s). Here, we assume that the attacker trains an OD model of different nature, Faster R-CNN [19]. The watermark verification results for each dataset in this scenario were as follows: VOC07, 100.0 ( $p$ : 2%,  $\delta$ : 1.05); TrafficSigns, 100.0 ( $p$ : 3%,  $\delta$ : 1.2); and CityPersons, 48.0 ( $p$ : 5%,  $\delta$ : 1.2). BBW performed completely on the VOC07 and the TrafficSigns dataset; however, it performed poorly on the CityPersons dataset. This is attributed to the poor OD performance of the extracted models (mAP50 11.74%). Since the MEA with Faster R-CNN fundamentally failed on this dataset, there was no longer a necessity to conduct watermark verification.

We expect BBW to become more effective as the attackers adopt more sophisticated model architectures. Such models are more capable of learning the heuristics of the target model, making it easier to learn a backdoor. For the same reason, BBW is expected to work effectively even against strong MEAs such that the extracted models faithfully reproduce the outputs of the target model.

### 7.3. Watermark Robustness to Countermeasures

**Weight Pruning** As weight pruning (WP) has been used for backdoor elimination in DNNs [14], we evaluated the robustness of our watermark to WP. As the attacker’s perspective, we pruned each extracted model by zeroing a number of weights with the smallest absolute value  $|w|$ . The results are presented in Fig. 6, showing that it is difficult to remove the watermark by WP without losing the OD capability of the extracted models. Note that although Liu *et al.* [14] have shown the effectiveness of naive WP for backdoor elimination, they also introduced a more sophisticated defense called *fine-pruning*. In our experiments, however, it severely degraded OD performance. The variation in these results might come from the difference in the models used in the experiments (they employed Faster R-CNN).

**Finetuning** Finetuning has also been used for backdoor elimination [20]. We assumed that the attacker has a substi-

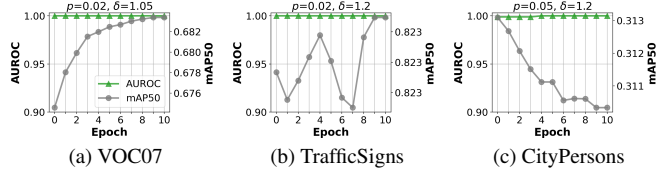


Figure 7. Watermark robustness to finetuning.

Dataset	Ratio	Poisoning Magnitude		
		1.05	1.1	1.2
		normal / adaptive		
<b>VOC07</b>	3%	100.0 / 72.11	100.0 / 86.33	100.0 / 95.22
<b>TrafficSigns</b>	3%	90.89 / 41.11	99.89 / 59.00	100.0 / 62.44
<b>CityPersons</b>	5%	96.44 / 83.33	99.0 / 85.78	99.89 / 87.11

Table 4. Watermark robustness to adaptive attacker.

tute dataset with clean BB annotations. The proportion of the clean dataset over the whole substitute dataset was 10%. Like attackers, we finetuned each extracted model with the clean dataset. Figure 7 presents the result of the watermarking verification on the finetuned models, showing that it is difficult to remove the watermark by finetuning as long as the finetuned model retains the OD capability.

**Adaptive Attacker** We consider an intermediate scenario for adaptive MEAs; we assume that the adaptive attacker trains an “odd BB detector” and applies it to query responses. The recall of the detector is assumed to be 80%, i.e., 20% of the trigger objects retain poisoned BBs. The results are presented in Table 4. As expected, our proposed watermark was mitigated by the adaptive attacker. However, the undetected trigger objects (20% of the trigger objects) still contributed to injecting a backdoor to the extracted models. We expect that the extracted models did not learn a backdoor of the given poisoning magnitude (i.e., 1.1) but still learned a smaller-scaled backdoor (e.g., 1.02) from the survived trigger objects. Let us emphasize that the capability of this adaptive attacker is strong. It is very challenging to obtain such a precise odd BB detector without the knowledge about the trigger cluster, whose rationale is discussed in Appendix:E.2.

## 8. Conclusion and Future Scope

This work presents a novel defense measure against MEAs on OD models, BBW, which involves poisoning BBs of the objects in API responses. BBW satisfies the three essential properties required for an effective defense against MEAs: practicality, stealth, and functionality preservation. Our future work includes proposing (i) a countermeasure for data-free MEAs and (ii) a guideline on how to tune the poisoning parameters according to model performance or attacker’s capability other than empirical ways.

## References

- [1] <https://github.com/giddyup/coco-minitrain>. 7
- [2] <https://openai.com/policies/business-terms>. 1
- [3] Yossi Adi, Carsten Baum, Moustapha Cisse, Benny Pinkas, and Joseph Keshet. Turning your weakness into a strength: Watermarking deep neural networks by backdooring. In *USENIX Security Symposium*, page 1615–1631, 2018. 1, 2
- [4] SelfDriving Car. Self-driving cars dataset. <https://universe.roboflow.com/selfdriving-car-qtywx/self-driving-cars-lfjou>, 2023. visited on 2024-08-01. 5
- [5] Shih-Han Chan, Yinpeng Dong, Jun Zhu, Xiaolu Zhang, and Jun Zhou. Baddet: Backdoor attacks on object detection. In *Computer Vision – ECCV 2022 Workshops*, pages 396–412, Cham, 2023. Springer Nature Switzerland. 1, 2, 3
- [6] Kangjie Chen, Xiaoxuan Lou, Guowen Xu, Jiwei Li, and Tianwei Zhang. Clean-image backdoor: Attacking multi-label models with poisoned labels only. In *ICLR*, 2023. 1, 2, 3
- [7] Yize Cheng, Wenbin Hu, and Minhao Cheng. Attacking by aligning: Clean-label backdoor attacks on object detection. *arXiv:2307.10487*, 2023. 2, 3
- [8] Marius Cordts, Mohamed Omran, Sebastian Ramos, Timo Rehfeld, Markus Enzweiler, Rodrigo Benenson, Uwe Franke, Stefan Roth, and Bernt Schiele. The cityscapes dataset for semantic urban scene understanding. In *CVPR*, 2016. 2
- [9] Martin Ester, Hans-Peter Kriegel, Jörg Sander, and Xiaowei Xu. A density-based algorithm for discovering clusters in large spatial databases with noise. In *KDD*, page 226–231, 1996. 5
- [10] M. Everingham, L. Van Gool, C. K. I. Williams, J. Winn, and A. Zisserman. The PASCAL Visual Object Classes Challenge 2007 (VOC2007) Results. <http://www.pascal-network.org/challenges/VOC/voc2007/workshop/index.html>. 5
- [11] Shafi Goldwasser, Michael P Kim, Vinod Vaikuntanathan, and Or Zamir. Planting undetectable backdoors in machine learning models. In *2022 IEEE 63rd Annual Symposium on Foundations of Computer Science (FOCS)*, pages 931–942, 2022. 1
- [12] Hengrui Jia, Christopher A. Choquette-Choo, Varun Chandrasekaran, and Nicolas Papernot. Entangled watermarks as a defense against model extraction. In *USENIX Security Symposium*, pages 1937–1954, 2021. 2
- [13] Yiming Li, Linghui Zhu, Xiaojun Jia, Yong Jiang, Shu-Tao Xia, and Xiaochun Cao. Defending against model stealing via verifying embedded external features. In *AAAI*, 2022. 1, 2
- [14] Kang Liu, Brendan Dolan-Gavitt, and Siddharth Garg. Fine-pruning: Defending against backdooring attacks on deep neural networks. In *RAID*, pages 273–294, 2018. 8
- [15] Chengxiao Luo, Yiming Li, Yong Jiang, and Shu-Tao Xia. Untargeted backdoor attack against object detection. In *ICASSP*, pages 1–5, 2023. 1, 2, 3
- [16] Hua Ma, Yinshan Li, Yansong Gao, Alsharif Abuadba, Zhi Zhang, Anmin Fu, Hyoungshick Kim, Said F. Al-Sarawi, Nepal Surya, and Derek Abbott. Dangerous cloaking: Natural trigger based backdoor attacks on object detectors in the physical world. *arXiv:2201.08619*, 2022. 2, 3
- [17] Hua Ma, Yinshan Li, Yansong Gao, Zhi Zhang, Alsharif Abuadba, Anmin Fu, Said F. Al-Sarawi, Surya Nepal, and Derek Abbott. Transcab: Transferable clean-annotation backdoor to object detection with natural trigger in real-world. In *42nd International Symposium on Reliable Distributed Systems (SRDS)*, pages 82–92, 2023. 1, 2, 3
- [18] Tribhuvanesh Orekondy, Bernt Schiele, and Mario Fritz. Prediction poisoning: Towards defenses against dnn model stealing attacks. *arXiv:1906.10908*, 2019. 1, 2
- [19] Shaoqing Ren, Kaiming He, Ross Girshick, and Jian Sun. Faster r-cnn: Towards real-time object detection with region proposal networks. *Advances in neural information processing systems*, 28, 2015. 8
- [20] Zeyang Sha, Xinlei He, Pascal Berrang, Mathias Humbert, and Yang Zhang. Fine-tuning is all you need to mitigate backdoor attacks. *arXiv:2212.09067*, 2022. 8
- [21] Anna Snarski, Walker L. Dimon, Keith Manville, and Michael Krumdick. Watermarking for data provenance in object detection. In *2022 IEEE Applied Imagery Pattern Recognition Workshop (AIPR)*, pages 1–7, 2022. 3
- [22] Sebastian Szyller, Buse Gul Atli, Samuel Marchal, and N. Asokan. Dawn: Dynamic adversarial watermarking of neural networks. In *ACM MM*, page 4417–4425, 2021. 1, 2, 3
- [23] Mingxing Tan and Quoc Le. Efficientnet: Rethinking model scaling for convolutional neural networks. In *International conference on machine learning*, pages 6105–6114. PMLR, 2019. 5
- [24] Florian Tramèr, Fan Zhang, Ari Juels, Michael K. Reiter, and Thomas Ristenpart. Stealing machine learning models via prediction apis. In *USENIX Security Symposium*, page 601–618, 2016. 1, 2
- [25] Jean-Baptiste Truong, Pratyush Maini, Robert J. Walls, and Nicolas Papernot. Data-free model extraction. In *CVPR*, pages 4771–4780, 2021. 7
- [26] Yusuke Uchida, Yuki Nagai, Shigeyuki Sakazawa, and Shin’ichi Satoh. Embedding watermarks into deep neural networks. In *ICMR*, page 269–277, 2017. 1, 2
- [27] Ultralytics. <https://github.com/ultralytics/ultralytics>. 5
- [28] Qixue Xiao, Yufei Chen, Chao Shen, Yu Chen, and Kang Li. Seeing is not believing: Camouflage attacks on image scaling algorithms. In *USENIX Security Symposium*, pages 443–460, 2019. 2
- [29] Jialong Zhang, Zhongshu Gu, Jiyong Jang, Hui Wu, Marc Ph. Stoecklin, Heqing Huang, and Ian Molloy. Protecting intellectual property of deep neural networks with watermarking. In *AsiaCCS*, page 159–172, 2018. 1, 2
- [30] Shanshan Zhang, Rodrigo Benenson, and Bernt Schiele. Citypersons: A diverse dataset for pedestrian detection. In *CVPR*, 2017. 5

Dataset	Num. Images (Num. Objects)			
	Training	Substitute-		Test
		training	finetuning	
<b>VOC07</b>	2,501 (7,844)	2,259 (7,012)	251 (806)	4,952 (14,976)
<b>TrafficSigns</b>	3,298 (3699)	692 (768)	77 (87)	602 (683)
<b>CityPersons</b>	2,276 (9,119)	450 (2,165)	50 (247)	699 (2,047)

Table A.1. Dataset statistics

## A. Datasets

### A.1. Dataset Description and Preparation

**VOC07** This dataset consists of common objects of 20 categories, including persons, animals, vehicles, and indoor items. We downloaded the dataset from <http://host.robots.ox.ac.uk/pascal/VOC/voc2007/>. We used the predefined training/val/test splits as the training/substitute/test sets in our experiments.

**TrafficSigns** This dataset consists of objects of 15 categories regarding traffic lights and traffic signs collected in self-driving scenarios. We downloaded the dataset from <https://www.kaggle.com/datasets/pkdarabi/cardetection>. We used the predefined training/val/test splits as the training/substitute/test sets in our experiments. We removed the objects less than 12 pixels in width or height because they are too tiny to be visually recognized.

**CityPersons** This dataset is a subset of the Cityscapes dataset [8], which consists of the following five categories: Pedestrian, Riders, Sitting Persons, Other Persons, and Group. We downloaded the images of the dataset from the website of the CityScapes dataset, <https://www.cityscapes-dataset.com/>, which is the parent dataset of the CityPersons dataset. We obtained the annotations of the CityPersons dataset from <https://github.com/cvgroup-njust/CityPersons/tree/master/annotations>. We split the predefined training set into the training and the test set for our experiments because the annotations of the original test set are not published. As the dataset contains city-view images captured in 18 cities, we treated the images of the following five cities as the test set: Stuttgart, Tübingen, Ulm, Weimar, and Zurich. The predefined validation split was used as the substitute set. Further, we removed the objects less than 30 pixels in width or height because they are too tiny to be visually recognized.

Table A.1 presents the statistics of the datasets. Basically, we respected the data splits predefined by the dataset providers as much as possible. As a result, the proportion of the data splits varied for each dataset. On the other hand, we believe it beneficial to evaluate the proposed method using data with different sizes.

### A.2. Key-set Preparation

We configured the key-set  $D_{key}$  of each dataset as follows: VOC07, a subset of the test split; TrafficSigns, the training split as is; and CityPersons, a subset of the training split. Let us emphasize that key-sets do not need to be annotated. Therefore, we supposed that demonstrating the effectiveness of our proposed watermark verification approach even on unannotated images would show its scalability. That is why we used the test set, which is not annotated in practice, as the key-set for the VOC07 dataset. However, for the TrafficSigns and the CityPersons dataset, we used their training splits as the key-sets because their test splits do not have sufficient numbers of trigger objects. Nevertheless, using a training set for a key-set is still reasonable because the owner of a target model must retain training samples. Furthermore, for the VOC07 and the CityPersons dataset, we used subsets of their base splits (VOC07  $\Rightarrow$  test split and CityPersons  $\Rightarrow$  training split) as the key-sets in order to save the computational time for watermark evaluation. Specifically, from the base split of each dataset, we sampled the images containing trigger objects and used the set composed of the sampled images as the key-set. Since trigger and nontrigger objects often coexist in a single image, the subset configured in this way can meet the requirement for a key-set that must contain both types of objects. The TrafficSigns dataset contains very few images where trigger and nontrigger objects coexist, so we used the original training split for the key-set without sampling.

## B. Models

### B.1. Training Hyperparameters

We used the default training parameters set by Ultralytics. A major exception was epoch size; we tuned it carefully for each combination of the datasets and the models so that model training terminates without overfitting. The configured epoch settings are as follows:

**VOC07:** target model, 200; benign and extracted models, 30; and finetuned models, 100.

**TrafficSigns:** all models, 50.

**CityPersons:** target model, 150 and other models, 100.

There are two additional minor exceptions.

*Learning rate for finetuning.* We set the learning rate for finetuned models to a small value of  $10^{-4}$  to keep the OD capability of extracted models inherited by target models.

*Epoch size for Faster R-CNN on CityPersons.* The epoch size for training extracted models on the CityPersons dataset had been set to 100. However, in the experiments with the Faster R-CNN (Sec. 7.2), we increased the epoch size to 200 because the epoch size of 100 was not sufficient. Even though, in the end, the accuracy of the extracted Faster R-CNN models was not satisfactory.

Dataset	Model		
	Target	Benign	Baseline
<b>VOC07</b>	70.75	71.35	67.38
<b>TrafficSigns</b>	96.60	82.34	82.41
<b>CityPersons</b>	37.38	30.53	31.57

Table B.2. OD performance (mAP50, %) of target, benign, and baseline model.

Dataset	Ratio	Num. (Percentage) of Trigger Objects			
		Training	Substitute-		Test
			training	finetuning	
<b>VOC07</b>	1%	81 (1.03%)	44 (0.69%)	11 (1.36%)	96 (0.64%)
	2%	162 (2.07%)	110 (1.71%)	30 (3.72%)	315 (2.10%)
	3%	234 (2.98%)	173 (2.73%)	37 (4.59%)	455 (3.04%)
<b>TrafficSigns</b>	1%	38 (1.03%)	9 (1.11%)	0 (0.00%)	15 (2.20%)
	2%	81 (2.19%)	20 (2.46%)	0 (0.00%)	30 (4.39%)
	3%	111 (3.00%)	26 (3.20%)	0 (0.00%)	33 (4.83%)
<b>CityPersons</b>	1%	95 (1.04%)	13 (0.72%)	3 (1.21%)	19 (0.93%)
	3%	290 (3.18%)	40 (2.22%)	7 (2.83%)	46 (2.25%)
	5%	459 (5.03%)	64 (3.55%)	12 (4.86%)	78 (3.81%)

Table C.3. Numbers (and percentages) of trigger objects in each data split.

## B.2. Model Performance

Table B.2 presents the OD performance of the target, the benign, and the baseline (nonwatermarked extracted) model. For the benign and the baseline model, the performance is averaged over the 30 models trained with different seeds.

## C. Trigger Objects and Watermarked Models

### C.1. Statistics of Trigger Objects

Table C.3 presents the statistics of the trigger objects in each data split of the experimental datasets. Here, only on the substitute-training splits, we counted the number of trigger objects determined from the target model’s predictions, not from the ground truth annotations. This reflects the poisoning ratios actually applied to the API responses to queries by the ME attackers in our experiments. To be more specific, the objects in the substitute-training split were cropped with their BBs predicted by the target model (not with their ground truth BBs) and fed into the trigger indicator function  $T$ . We also note that the substitute-finetuning set of the TrafficSigns dataset does not contain trigger objects. Therefore, the experiment of the watermark robustness evaluation to finetuning on this dataset (Sec. 7.3) reflects the situation where attackers do not have images containing trigger objects.

### C.2. Statistics of Key-set

Table C.4 presents the statistics of the key-set  $D_{key}$  for each dataset. In addition, Table C.5 presents the statistics of paired objects in the key-sets, where the paired object is the

Dataset	Ratio	Numbers of:		
		Images	Trigger Obj.	Nontrigger Obj.
<b>VOC07</b>	1%	59	90	365
	2%	279	322	584
	3%	365	449	795
<b>TrafficSigns</b>	1%	3298	50	3772
	2%	3298	96	3726
	3%	3298	135	3687
<b>CityPersons</b>	1%	69	94	480
	3%	208	291	1359
	5%	324	507	2141

Table C.4. Numbers of images, trigger objects, and nontrigger objects in key-sets.

Dataset	Ratio	Magnitude							
		0.8	0.9	0.95	1.0	1.05	1.1	1.2	
<b>VOC07</b>	1%	$ \mathcal{V} $	30	32	32	32	31	32	
		$ \mathcal{V}^c $	259	260	259	261	258	258	
	2%	$ \mathcal{V} $	226	311	313	311	311	309	284
		$ \mathcal{V}^c $	429	432	432	433	432	432	427
	3%	$ \mathcal{V} $	276	427	428	428	428	424	376
		$ \mathcal{V}^c $	576	587	590	590	590	585	581
<b>TrafficSigns</b>	1%	$ \mathcal{V} $	22	25	25	27	26	28	28
		$ \mathcal{V}^c $	3192	3193	3197	3194	3194	3191	3191
	2%	$ \mathcal{V} $	42	47	50	51	51	53	51
		$ \mathcal{V}^c $	3171	3174	3169	3169	3166	3175	3169
	3%	$ \mathcal{V} $	67	74	78	80	81	81	80
		$ \mathcal{V}^c $	3134	3136	3136	3140	3139	3141	3142
<b>CityPersons</b>	1%	$ \mathcal{V} $	30	29	29	30	31	31	31
		$ \mathcal{V}^c $	259	257	257	259	265	261	262
	3%	$ \mathcal{V} $	106	106	106	106	107	107	105
		$ \mathcal{V}^c $	750	750	755	750	753	751	752
	5%	$ \mathcal{V} $	187	189	190	189	190	186	183
		$ \mathcal{V}^c $	1199	1200	1201	1196	1204	1199	1193

Table C.5. Average cardinality of  $\mathcal{V}$  (set of paired trigger objects) and  $\mathcal{V}^c$  (set of paired nontrigger objects) for each poisoning configuration, where  $\eta = 0.7$ .

one satisfies the condition Eq. (5). We counted paired objects between the target model and the extracted models of each poisoning configuration. The numbers in the table are averaged over 30 extracted models of each configuration.

The threshold  $\eta$  (Eq. (5)) was fixed to 0.7 throughout our experiments, but we also confirmed that  $\eta$  was not sensitive to watermarking verification performance. We conducted experiments while varying  $\eta$  in  $\{0.5, 0.6, 0.7, 0.8, 0.9\}$  on the VOC07 dataset with the poisoning ratio of 2% and the poisoning magnitude of 1.1. All the settings achieved 100% verification.

### C.3. Watermarked Model Performance

Table C.6 presents the OD performance of the watermarked models. For each poisoning configuration, the performance is averaged over 30 models trained with different seeds.

Dataset	Ratio	Magnitude					
		0.8	0.9	0.95	1.05	1.1	1.2
VOC07	1%	67.49	67.43	67.40	67.46	67.47	67.41
	2%	67.28	67.45	67.39	67.46	67.40	67.42
	3%	67.27	67.51	67.44	67.38	67.32	67.43
TrafficSigns	1%	82.10	82.34	82.28	82.26	82.23	82.28
	2%	82.32	82.49	82.20	82.22	82.23	82.31
	3%	82.14	82.25	82.28	82.28	82.32	82.51
CityPersons	1%	31.53	31.51	31.52	31.54	31.45	31.50
	3%	31.54	31.46	31.45	31.56	31.55	31.49
	5%	31.28	31.36	31.53	31.41	31.56	31.31

Table C.6. OD performance (mAP50, %) of watermarked extracted models

Dataset	Ratio	Poisoning Magnitude						
		0.8	0.9	0.95	1.0	1.05	1.1	1.2
VOC07	1%	19.22	20.89	18.22	17.22	21.22	16.33	23.33
	2%	100.0	100.0	100.0	49.78	100.0	100.0	100.0
	3%	100.0	100.0	100.0	66.22	100.0	100.0	100.0
TrafficSigns	1%	91.33	93.22	91.44	90.33	90.67	91.11	97.22
	2%	95.22	91.78	93.33	86.67	94.33	96.56	99.0
	3%	99.78	100.0	98.33	95.22	98.11	100.0	100.0
CityPersons	1%	59.11	66.33	61.11	69.33	58.22	61.78	67.56
	3%	35.67	41.11	45.33	54.67	58.0	64.44	71.67
	5%	30.22	33.11	27.44	59.78	63.67	81.0	88.89

Table D.7. Watermark verification accuracy (AUROC, %) using suspiciousness score based on IoU-based inconsistency metric. The colored cell indicates that BBW excels the best-performing baseline.

## D. Additional Results

### D.1. Results with IoU-based Inconsistency Metric

Table D.7 presents the results of the watermark verification using the suspiciousness score based on the IoU-based inconsistency metric (Eq. (7)).

### D.2. Watermark Visualization

Figure D.1 presents examples of prediction results by the target, the benign, and the extracted model on the TrafficSigns and the CityPersons dataset.

## E. Supplemental Figures and Discussion

### E.1. Distribution of Trigger Objects

Figure E.1 visualizes the scatter plots of object features (*i.e.*  $E(o)$ ). The features were decomposed into the two-dimensional space by using UMAP (<https://umap-learn.readthedocs.io/en/latest/>). We can confirm that the trigger objects of the compact cluster are densely distributed.

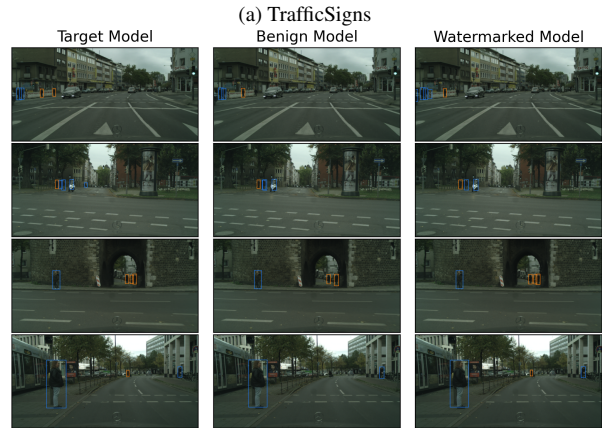


Figure D.1. Visualization of our proposed watermark on (a) the TrafficSigns and (b) the CityPersons dataset. Refer to Fig. 4 for the caption.

### E.2. Discussion on Adaptive Attacker

This small section discusses how difficult it is for adaptive attackers to train a precise “odd BB detector”. We evaluated the IoU-based BB inconsistencies (Eq. (7)) between API responses with BB poisoning applied and clean labels (*i.e.* ground truth BB annotations) for both trigger and non-trigger objects. The settings were as follows: dataset, VOC07; poisoning ratio, 3%; and poisoning magnitude, 1.1. The result is presented in Fig. E.2. Indeed, trigger objects exhibit a certain degree of difference in their BBs from the clean labels, as illustrated in the orange histogram. This may give

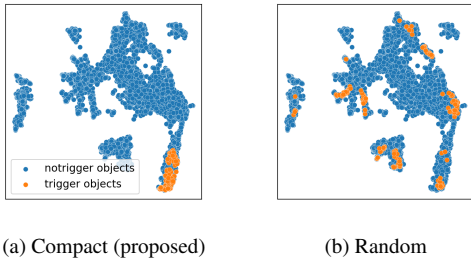


Figure E.1. 2-D visualization of object features for each cluster type: (left) compact cluster and (right) random cluster (dataset: VOC07, poisoning ratio: 3%). The blue and the orange dots indicate the nontrigger and the trigger objects, respectively.

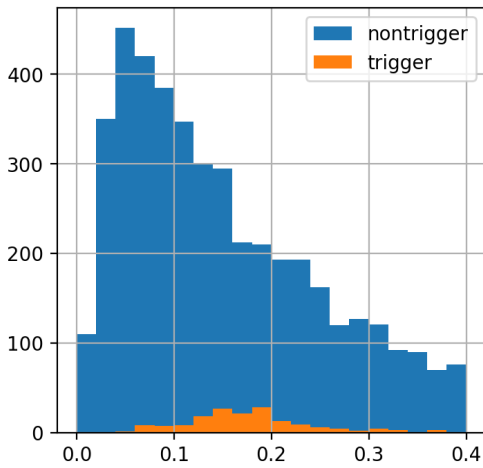


Figure E.2. IoU-based BB inconsistencies (Eq. (7)) between API responses with BB poisoning applied and clean labels.

the attacker a hint to establish an odd BB detector. However, as shown in the blue histogram, non-trigger objects also display some differences. This indicates that even if attackers had clean annotations for the substitute data, it would be challenging to precisely separate trigger objects from API responses. Therefore, it is difficult for adaptive attackers to train a precise odd BB detector.